Thin Structure of Near-Field Emission of Semiconductor Laser

K.P.Gaikovich, V.F.Dryakhlushin
Institute for Physics of Microstructures RAS, GSP-105 Nizhny Novgorod – 603950, Russia

ABSTRACT

A near-field structure of the semiconductor laser emission is revealed using image deconvolution of SNOM measurements. The comparison with the atomic-force microscope measurements of the emitting surface relief shows that inhomogeneities of this structure are likely related to nano-scale inhomogeneities of the emitting laser surface. To retrieve the true structure of near-field laser emission taking into account the probe transfer function, the image deconvolution method based on the Tikhonov's method of generalized discrepancy was used. As a result, in the SNOM measurements small (3-4%) variations with a spatial size of about 50 nm have been discerned.

Keywords: semiconductor laser, near-field emission, image deconvolution, emitting surface relief

1. INTRODUCTION

Results of SNOM measurements analysis of a near-field structure of the semiconductor laser emission are presented. In contrast to papers in this area [1-3] we have achieved a higher resolution that makes it possible to observe thin inhomogeneities of near-field laser emission, which are likely related to nano-scale inhomogeneities of the emitting laser surface. To achieve such a resolution, a small-aperture probe [4] shown in Fig.1 has been used in a SNOM system. The microscope resolution is determined by the size of the probe aperture (~50-100 nm), which is much smaller than the wavelength of light. It was possible to discern in SNOM laser emission images small, comparable to the probe size, inhomogeneities of structure, the true size of which is inevitable smoothed by the probe transfer function and the true magnitude is inevitable decreased. To retrieve the true structure of near-field laser emission, the Tikhonov's method of generalized discrepancy based on the Tikhonov's theory of ill-posed problems [5] was used. To test this method, numerical modelling has been carried out and measurements results have been processed taking into account the probe transfer function determined from the test measurements with the etched vanadium film. Then, image deconvolution method is applied to retrieve images of the near-field emission of semiconductor laser distorted by the instrument transfer function influence. Using this approach, in the SNOM measurements small (3-4%) variations with a spatial size of about 50 nm have been discerned. Retrieved images are compared to measurements of the laser emitting surface relief obtained using atomic-force microscope.

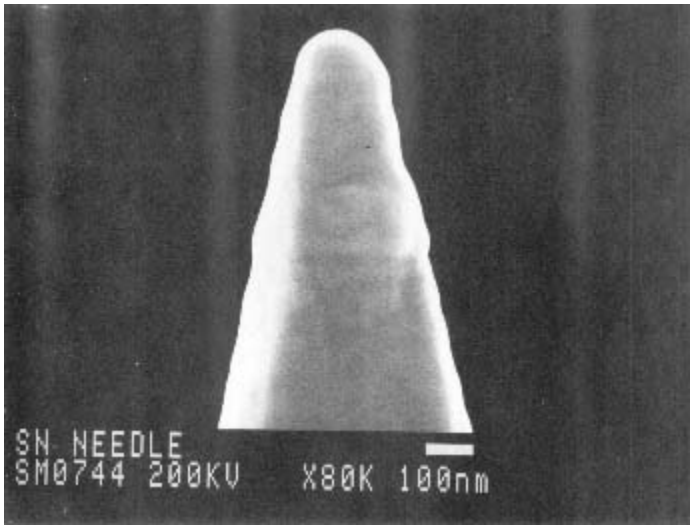

Fig. 1. The SNOM probe.

2. IMAGE DECONVOLUTION AND NUMERICAL MODELLING

2.1 Integral equation and transfer function

If a 2-D distribution of SNOM signal is measured, then it can be (at least, approximately) expressed as a 2-D convolution of true distribution and probe transfer function

$$z_{\mathrm{m}}(x,y) = \int_{-\infty}^{+\infty}\int_{-\infty}^{+\infty} K(x-s,y-t)z(s,t)dsdt \qquad (1)$$

where the kernel $K(w,W)$ is the transfer function, $z_{\mathrm{m}}(x,y)$ is the measured signal, $z(s,t)$ is the true distribution to be found. The solution of (1) relative to $z(s,t)$ make it possible to retrieve the surface image with a higher resolution.

The key part of our approach is a method of determination of the transfer function in (1) from the image of a structure that contains small (much less than the size of aperture) details. These details can be considered as δ-functions, so one has from (1) the form of the kernel:

$$z_m(x,y) = K(x,y). \qquad (2)$$

In our research the probe transfer function has been determined from the analysis of a test structure (thin vanadium film (<10 nm) on the quartz partially etched to the substrate), and it was obtained that really, all the smallest details of the measured image are similar. The corresponding kernel is determined from (2), and it can be well approximated by the 2D Gauss distribution with half-width parameters $\sigma_x = \sigma_y = \sigma \cong 70$ nm. The achieved (after the deconvolution) resolution $\sigma_r \cong 20$ nm (or about 0.045 of the SNOM wavelength) has been determined by the Gaussian approximation of smallest details of the retrieved image. In Fig.2 one can see two examples of such small details measured on the test etched vanadium film on the quartz substrate.

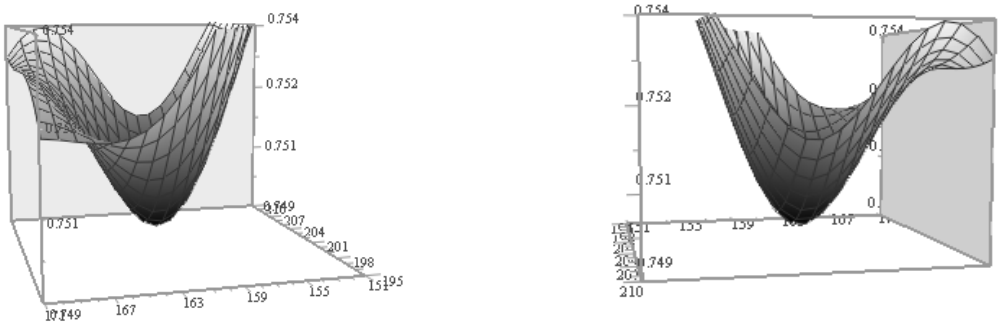

Fig. 2. Two examples of the smallest details of the SNOM image of etched vanadium film.

In is easy to see that these details have practically the same form, so they can be used as the probe transfer function in the further analysis.

The equation (1) is an integral Fredholm equation of the 1st kind, the solution of which is an ill-posed problem. To solve ill-posed problems various regularization methods are in use. These methods use the available additional a priori information about an exact solution. In this paper Tikhonov's method of image deconvolution based on the generalized discrepancy principle is used to retrieve a structure of near-field semiconductor laser emission. This method uses the information that the exact solution belongs to the set of square integrable functions that have generalized square-integrable derivatives. It is very suitable for continuous functions. An important advantage of the considered method is the convergence (in W_2^2 –space, and, hence, uniformly [5]) of the approximate solution to an exact solution at the decrease of measurement errors. The values of the measurement error parameter δ (estimated in L_2- space) and the kernel error parameter h are the only parameters of the Tikhonov's method of the generalized discrepancy. They determine a quality of the retrieval by implicit relation with the

regularization parameter, on the value of which depends an extent of the smoothing of an approximate solution. At $\delta \to 0$, $h \to 0$ the retrieved distribution converges uniformly to the exact one. So, there is no need in the use of large statistical ensembles to obtain a representative estimation of the accuracy of retrieval (as it is necessary in other methods with an integral or mean-square convergence) – it is enough to make a numerical modeling for typical and, may be, for extreme distributions.

2.2 Tikhonov's method of deconvolution

The equation (1) is the Fredholm integral equation of the first kind. Its solution z^α gives an approximate retrieval of the true distribution. The measure of the measurement error δ and the measure of the kernel error h satisfy to

$$\|z_m - z\|_{L_2} \le \delta, \qquad \|K - K_h\|_{W_2^2 \to L_2} \le h, \tag{3}$$

where z is an exact solution. According to generalized discrepancy Tikhonov's method, an approximate solution of (1) is obtained from the condition of the minimum of the generalized discrepancy functional

$$M_\alpha[z^\alpha] = \|K_h z^\alpha - z_m\|_{L_2}^2 + \alpha \|z^\alpha\|_{W_2^2}^2 \tag{4}$$

at the additional condition that is the generalized discrepancy principal itself:

$$\|K_h z^\alpha - z_m\|_{L_2}^2 = (\delta + h\|z^\alpha\|_{w_2^2})^2. \tag{5}$$

Using the property of the Fourier transform, one has:

$$z^\alpha(s,t) = \frac{1}{4\pi^2} \int_{-\infty}^{+\infty}\int_{-\infty}^{+\infty} \frac{\tilde{K}_h^*(\omega,\Omega)\tilde{z}_m^*(\omega,\Omega)e^{i(\omega s+\Omega t)}d\omega d\Omega}{L(\omega,\Omega) + \alpha[1+(\omega^2+\Omega^2)^2]} \tag{6}$$

where $\tilde{K}_h^*(\omega,\Omega) = \tilde{K}_h(-\omega,-\Omega), \qquad L(\omega,\Omega) = |\tilde{K}_h(\omega,\Omega)|,$

$$\tilde{z}_m^*(\omega,\Omega) = \int_{-\infty}^{+\infty}\int_{-\infty}^{+\infty} z_m(x,y)e^{-i(\omega x+\Omega y)}dxdy, \tag{7}$$

$$\tilde{K}_h(\omega,\Omega) = \int_{-\infty}^{+\infty}\int_{-\infty}^{+\infty} K_h(u,w)e^{-i(\omega u+\Omega w)}dudw, \tag{8}$$

It is very important that these formulas can be calculated using Fast Fourier Transform to overcome the well-known difficulties of calculations for large-dimensional images.

2.3 Numerical modeling

It is well known that the accuracy of the retrieval in ill-posed problems can be determined on the basis of the numerical simulation only using the closed-circuit scheme: at first, an initial distribution is given, then, using this distribution, an exact left side of (1) is calculated, then a random error is added to obtain "measurements data" and, finally, the equation (1) is solved and results are compared with the initial distribution.

The results of numerical modelling at various values of δ are shown in Figs.3-5. The value of the kernel error parameter was assumed $h = 0$. The assumed error level for the case shown in Fig.4 (left) is close to this in real SNOM experiment. The retrieval results shown in Fig.4 (right) are obtained for the assumed error level 4 times less. One can see the convergence to the exact solution at the decrease of the assumed level of measurement errors, so there is a real possibility to overcome the resolution limit related to the smoothing property of the probe transfer function. In Fig.5 (left) "measurements data" are shown that are distorted by a random noise that is 10 times more than the real measurements error. This noise is uncorrelated between neighbour pixels. It is easy to see that the quality of retrieval is quite satisfactory even at this high level of

random noise. The corresponding result of retrieval is given in Fig.4 (right). In the numerical modeling we use in the equation (1) the transfer function in the form of 2D Gauss distribution at above-mentioned values of parameters $\sigma_x = \sigma_y = \sigma \cong$ 70 nm:

$$K(x,y)=\frac{1}{\pi\sigma_x\sigma_y}\exp\left(-\frac{(x-x')^2}{\sigma_x^2}-\frac{(y-y')^2}{\sigma_y^2}\right) \tag{9}$$

and measured SNOM images of test vanadium film. The smoothed by the probe transfer function images are calculated using the 2D convolution equation (1), and, then, we add the random noise with the proper rms value to obtain "measurements data".

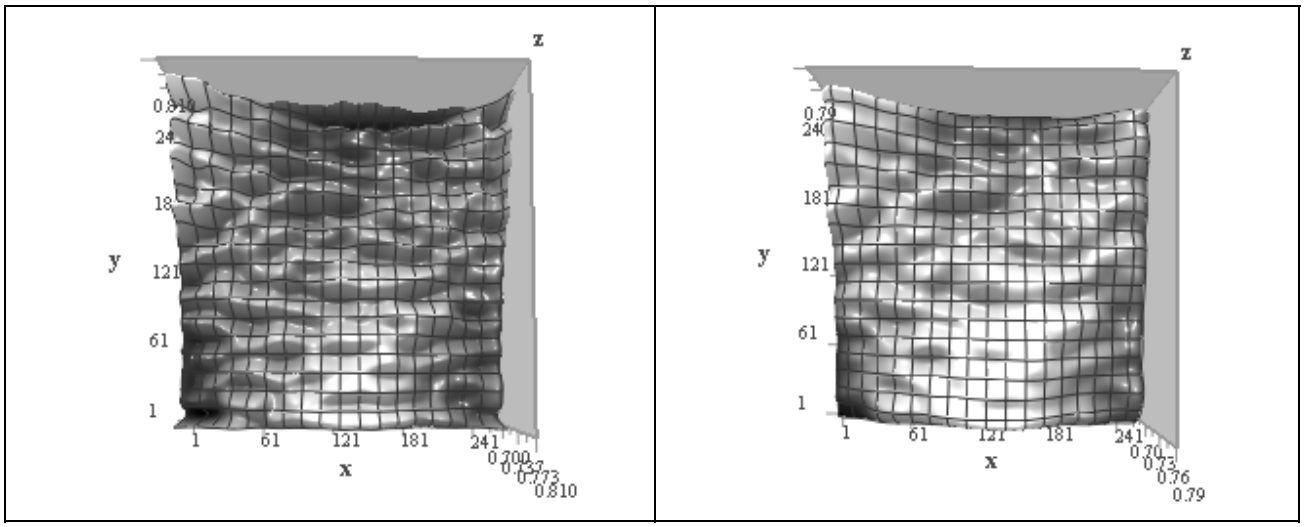

Fig. 3. Numerical modelling. Initial SNOM image z(x,y) (leftr) and calculated "measurement data" $z_m(x,y)$ in (1) (right).

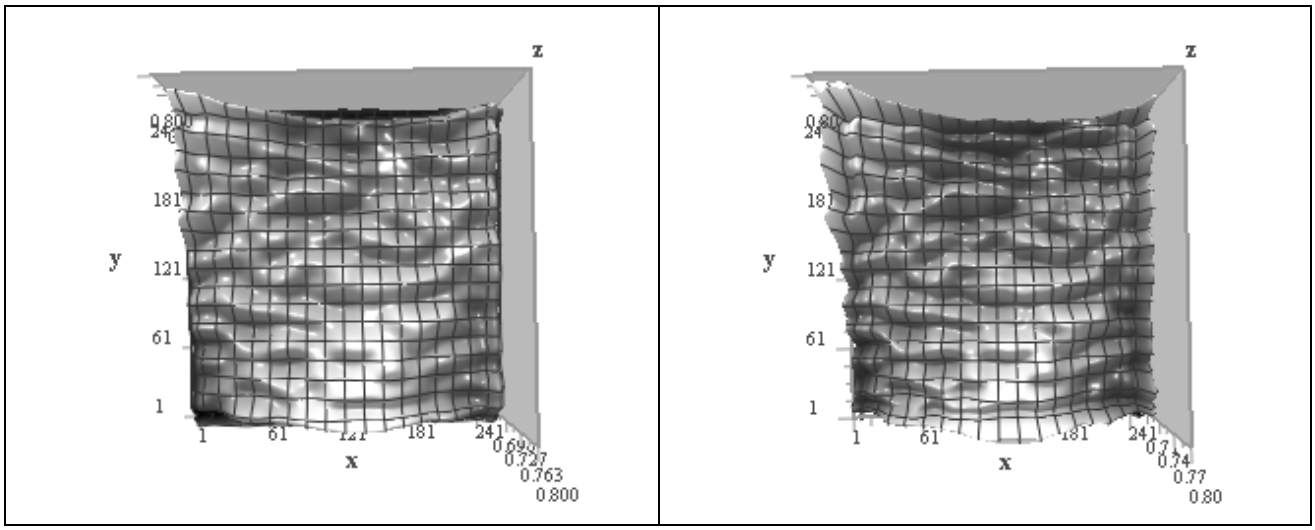

Fig. 4.Results of retrieval by "measurement data"(see in Fig.3, right):
at the real SNOM error level (left) and at 4 times less error level (right).

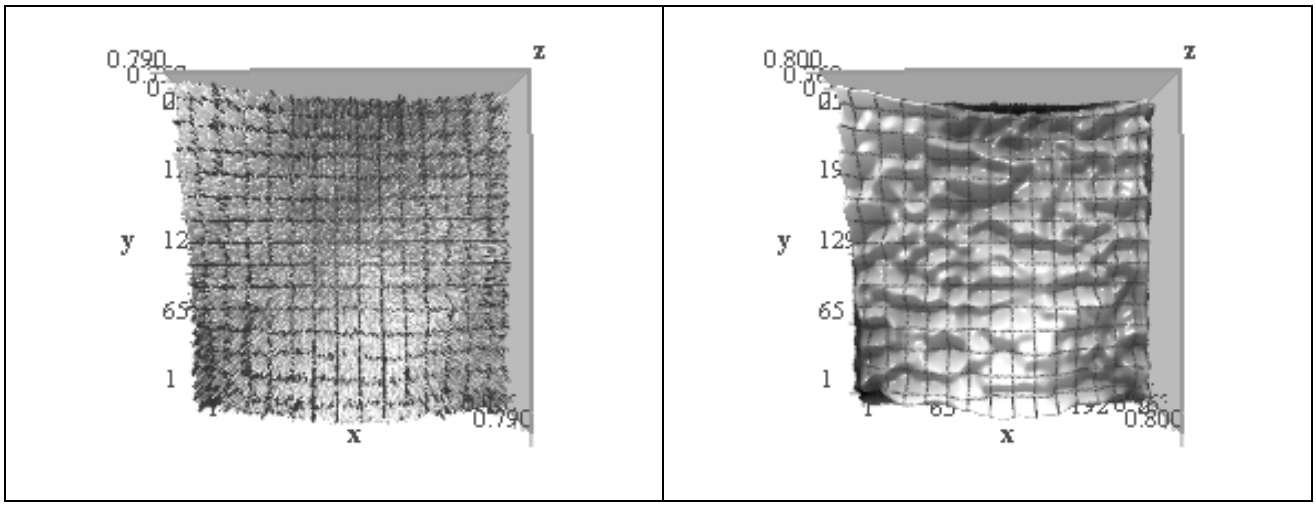

Fig. 5. "Measurements data" with a large uncorrelated random error (left). Results of retrieval (right).

2.4 Study of the deconvolution method using a test film sample

Using the developed method measured SNOM images of the test vanadium film have been processed. The test sample was a very thin vanadium film (<10 nm) on the quartz partially etched to the substrate. The initial image was obtained with the help of the scanning near-field optical microscope "Aurora" by "Topometrix" firm, operating at wavelength of optical radiation of 488 nm; the transmission coefficient of the probe was $4 \cdot 10^{-3}$. The noise level (parameter of Tikhonov's method that determines the value of regularization parameter) was 0.03 mV. In Fig. 6 the results of retrieval of SNOM-images are shown. It is obvious that the resolution of retrieved image is much better and the edge of the test sample is more clearly seen.

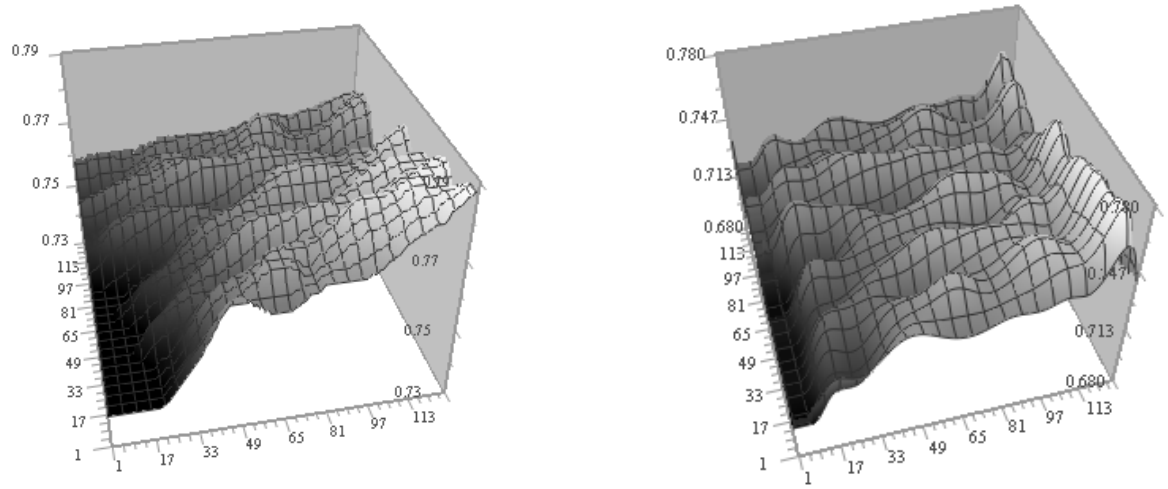

Fig. 6. Measured (left) and retrieved (right) SNOM-images of the test vanadium film (in mV). The pixel size is 3.3 nm..

At this level of measurements accuracy the achieved resolution σ_r in retrieved images is at least 3 times better than the resolution in initially measured images. The achieved resolution σ_r can be determined by the smallest details of the retrieved image in the same way as the resolution of the initial image σ in (2). So, we obtain $\sigma_r \cong 22$ nm, or about 0.045 of the SNOM wavelength. In Fig.7 the measured and retrieved images are shown in a larger area. The achieved results are very suitable for our goal to study the inhomogeneities of the near-field emission of the semiconductor laser. It should be mentioned that the similar approach to the image deconvolution we used in some different applications [6-13], including radiometry imaging, scanning tunneling microscopy and study of 2D current distributions on high-temperature superconductors films by measurements of 2D distribution of magnetic field measured above the film surface.

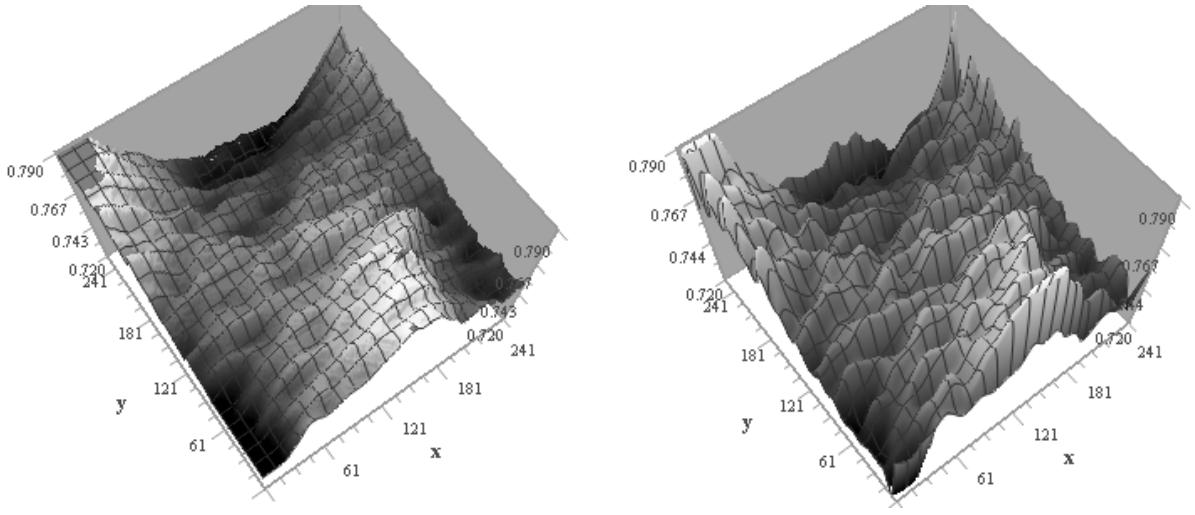

Fig. 7. Measured (left) and retrieved (right) SNOM-images of the test vanadium film for a larger area (in mV). The pixel size is 3.3nm.

3. MEASUREMENTS AND PROCESSING OF NEAR_FIELD EMISSIOM OF SEMICONDUCTOR LASER

Using SNOM microscopy and image deconvolution method the semiconductor injection laser with quantum walls has been studied. It has a current threshold of 0.5 A, quantum efficiency of 27% at power of 0.2 W on the wavelength λ=961 nm. The working width of the active region of the laser consisted 100 μm. The laser scheme is shown in Fig.8

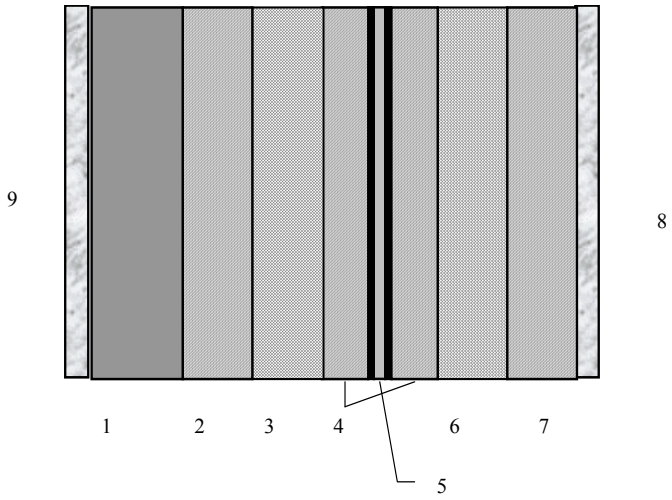

Fig.8. Structure of the laser. 1 – substrate n^+ - GaAs, 2 – buffer layer GaAs (550 nm), 3- bounding layer n - InGaP (500 nm), 4 – wave-guide layers GaAs (300 nm), 5 – active region consisting of two quantum walls InAs (8 nm) and separating layer GaAs (80 nm), 6 – bounding layer p – InGaP (500 nm), 7 – contact layer p^+ - GaAs, 8,9 – ohmic Au contacts to n and p – type of GaAs respectively

Results of SNOM measurements in collection mode of the near-field (the probe-surface distance $h \leq 5$ nm $<< \lambda$) laser emission are shown in Fig.9, Fig.10 (left). There are small spatial variations of the emission in this image (Fig.9), but taking into account the averaging over the probe transfer function footprint, after the image deconvolution, we have obtained the true emission distribution shown in Fig.10 (right). The variations in this reconstructed image are much more pronounced (about 3-4%). The size of spatial variations of the laser emission is about 50 nm, and these variations are most likely related to nano-scale inhomogeneities of the emitting surface, a structure of which measured by an atomic-force microscope is shown in Fig.11.

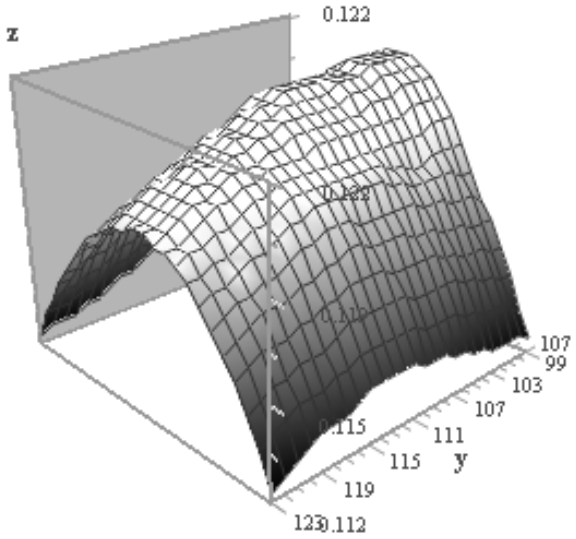

Fig.9. SNOM measurements of the near-field emission of the semiconductor laser. The pixel size is 10 nm.

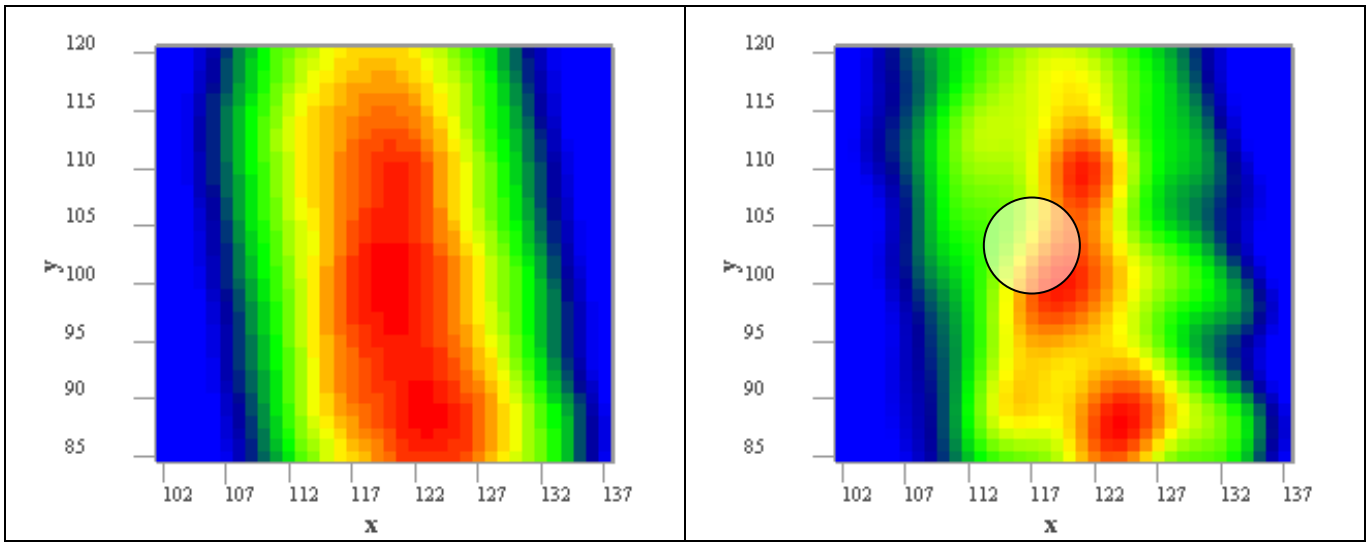

Fig.10. Initial (left) and reconstructed (right) SNOM-images of near-field laser emission. The circle in the reconstructed image marks the probe pattern footprint. The pixel size is 10 nm.

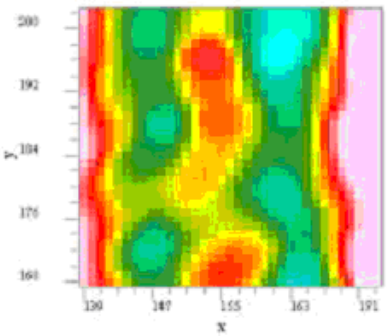

Fig.11. Relief of the emitting surface of the laser measured by an atomic-force microscope (pixel size is 4,3 nm).

4. CONCLUSION

The SNOM measurements analysis of a thin near-field structure of the semiconductor laser emission is presented. Similar research have been published before [1-3], but now, in the study results of which are presented in this paper, we have achieved a higher resolution to observe more thin, nano-scale, inhomogeneities of near-field laser emission, which are likely related to nano-scale inhomogeneities of the emitting laser surface. To achieve such a resolution, a small-aperture probes developed in our institute [4] with the effective size of 50-100 has been used in a SNOM system and the Tikhonov's method of generalized discrepancy [5] based on the Tikhonov's theory of ill-posed problems was applied to make the resolution yet better. To test this method, numerical modelling has been carried out and measured images of the test sample (the etched vanadium film on the quartz substrate) have been processed taking into account the probe transfer function determined from the smallest details of the same measured images of the film. Because these details had about the same form, they were considered as responses of the microscope on δ-function, so this form could be considered as the transfer function in the corresponding integral 2D convolution equation that related measured and true images.

Then, the developed method of image deconvolution is applied to retrieve images of the near-field emission of semiconductor laser distorted by the instrument transfer function influence. Using this approach, in the SNOM measurements small (3-4%) variations with a spatial size of about 50 nm have been discerned. Retrieved images are compared to measurements of the laser emitting surface relief obtained using atomic-force microscope and it was obtained that the surface inhomogeneities have the similar typical size, so it is very likely that the origin of the near-field inhomogeneities of the emission of the semiconductor laser is related to the emitting surface relief.

These results show that near-field measurements of the emission of semiconductor lasers give useful information about the emission formation near the emitting surface. May be, using the possible relation of the near-field emission inhomogeneities with corresponding inhomogeneities of the emitting surface of the laser one could form an arbitrary distribution of the near-field laser emission in various possible applications, for example, in remote control systems. Further study should include the investigation of the height dependence of the laser emission. The developed approach can be also useful for the study of multi-mode semiconductor laser emission to determine the mode distribution over the emitting surface.

Acknowledgement

This work was supported by Russian Fond for Basic Research (grants No. 01-02-16432 and 03-02-17321) and by grant of INTEL.

REFERENCES

1. J.Kim, J.T.Boyd, H.E.Jackson, K.D.Choquette. *Applied Physics Letters*, 2000, vol.76, *No*.5, pp.526-528.
2. D.K.Young, M.P.Mack, A.C.Abare, and al. *Applied Physics Letters*, 1999, vol.74, *No*.16, pp.2349-2351.
3. J.Kim, D.E.Pride, J.T.Boyd, and H.E.Jackson. *Applied Physics Letters*, 1998, vol.72, *No*.24, pp.3112-2351.
4. V.F.Dryakhlushin, A.Yu.Klimov, V.V.Rogov, and S.A.Gusev. *Instruments and experimental techniques*, 1998, vol.41, *No*.2, pp.139-139.
5. A.N.Tikhonov, Solution of ill-posed problems. New York, Winston, 1977.
6. Gaikovich K.P., Zhilin A.V. Radiophysics and Quantum Electronics, 1999, vol.42, *No.*10, pp.825-833. Kluwer Academic/Plenum Publishers.
7. Gaikovich K.P., Nozdrin Ju.N., Zhilin A.V. Conference *Proceedings of 2000 2nd Intern. Conf. on Transparent Optical Networks (ICTON 2000, Gdansk, Poland, June 5-13, 2000)*, 2000, Gdansk: IEEE, pp.173-175.
8. K.P.Gaikovich, Yu.N.Nozdrin, A.N.Reznik, and V.L.Vaks. *Physics of Low-Dimensional Structures*, 2002, vol.5/6, pp.99-104.
9. Gaikovich K.P., Gribkov B.A., Mironov V.L., Treskov S.A., Zhilin A.V. *Proceedings of International Workshop "Scanning Probe Microscopy – 2002' (Nizhny Novgorod, March 3-6, 2002)*, 2002, Institute for Physics of Microstructures RAS, pp. 255-257.
10. Gaikovich K.P., Gribkov B.A., Mironov V.L., Treskov S.A., and Zhilin A.V. *Physics of Low-Dimensional Structures*, 2002, vol.5/6, pp.85-92.
11. Gaikovich K.P., Mironov V.L., Zhilin A.V. *Physics of Low-Dimensional Structures*, 2003, vol.3/4, pp.251-256.
12. Gaikovich K.P., Nozdrin Yu.N., Reznik A.N., Zhilin A.V. *XII German–Russian–Ukrainian Seminar on High Temperature Superconductivity (25-29 October, 1999, Kiev, Ukraine)*, 1999, Kiev: V.N.Bakul Institute for Superhard Materials of National Academy of the Ukraine, p.86.
13. Gaikovich K.P., Nozdrin Yu.N., Zhilin A.V. *Central European Journal of Physics*, 2003, No.3, pp.363-392.